refinement or results. In the present instance, either Sn_4^{2-} or $Sn_2Bi_2^{2-}$ (disordered) produced a very satisfactory solution, with convergence at $R = 0.094$ and $R_w = 0.115$ for the former and $R = 0.088$ and $R_w = 0.107$ for the latter. Though the latter is of course significantly lower, a large part of this improvement arose from a better fit of the anomalous dispersion correction. Compared with those of other polyatomic anion and crypt structures, the agreement factors were better than average for either model. The final difference map, normally used as a concluding test for discrepancies in the final solution, was if anything cleaner for Sn_4^{2-} than for $Sn_2Bi_2^{2-}$.

The only crystallographic indication that the former model was incorrect is the fact that the thermal parameters for the crypt atoms (average $B = 10.8$ Å^2) were much larger than those found for the heavier anion atoms (8.2 Å^2). On the other hand, the values were relatively close, 8.3 and 8.7 Å^2, respectively, for the disordered $Sn_2Bi_2^{2-}$ model. Since the heavy atoms for the most part determine the structure, the mistake of assigning too small of a scattering factor for the anion atoms in the Sn_4^{2-} model was in effect simply compensated for by a decrease in the overall scale factor and an increase in light-atom thermal parameters. Thus the error in the heavy atoms showed up only in the light atoms. Of course, the problem is moot in this case as a conventional analysis was performed, but sometimes this is not possible when reactions produce very small quantities and multiphase products.

Acknowledgment. We thank Professor R. A. Jacobson and his group for advice and assistance with the structure determination.

Registry No. (2,2,2-crypt-K^+)$_2Sn_2Bi_2^{2-}$·en, 82167-47-3; KSnBi, 82150-33-2; K_3Bi_2, 12598-61-7; KSn_2, 82150-34-3.

Supplementary Material Available: Listings of light-atom bond distances and angles for the cations (Table III) and structure factor amplitudes (13 pages). Ordering information is given on any current masthead page.

Contribution from Ames Laboratory—DOE[1] and Department of Chemistry,
Iowa State University, Ames, Iowa 50011

Two Zirconium Iodide Clusters. Hexazirconium Dodecaiodide (Zr_6I_{12}) and Cesium Hexazirconium Tetradecaiodide ($CsZr_6I_{14}$)

DENNIS H. GUTHRIE and JOHN D. CORBETT*

Received January 5, 1982

Gem- or rod-shaped crystals of the title compounds are obtained from the reaction of ZrI_4, excess Zr strips and, for the latter, CsI at 850–925 °C for 15–40 days in welded tantalum containers. The structures of both were determined from diffraction data collected on a four-circle diffractometer with Mo Kα radiation at room temperature. Zr_6I_{12} (γ-ZrI_2) ($R\bar{3}$, $a = 14.502$ (2) Å, $c = 9.996$ (2) Å, $Z = 3$) contains a slightly compressed metal antiprism (d(Zr–Zr) = 3.204 (2) and 3.194 (1) Å) in which the six iodine atoms bridging waist edges of the metal antiprism also occupy exo positions in six other clusters, giving the representation $Zr_6I^i_6I^{i\text{-}a}_{6/2}I^{a\text{-}i}_{6/2}$ (i = inner, a = outer). Extended Hückel calculations support the notion that trigonal distortion of the metal cluster is responsible for its diamagnetism. The structure of $CsZr_6I_{14}$ (*Cmca*, $a = 15.833$ (2) Å, $b = 14.300$ (3) Å, $c = 12.951$ (2) Å, $Z = 4$) is derived from that known for Nb_6Cl_{14} and Ta_6I_{14} by addition of cesium to a large interstice. The unsymmetric bridging in $Cs(Zr_6I^i_{10}I^{i\text{-}a}_2I^a_{4/2})$ produces a tetragonally distorted metal octahedron with average distances of 3.29 Å (×8) and 3.35 Å (×4). The two structures also consist of approximately ccp M_6X_{12} units, with cesium in all octahedral holes in the latter. These and some related phases may also be described systematically in terms of close-packed halogen layers containing ordered vacancies, interstitials, and clusters of metal atoms in octahedral holes.

Introduction

Although (Nb, Ta)$_6X_{12}^{n+}$ and (Mo, W)$_6X_8^{m+}$ clusters with X = Cl, Br, I have been well-known for some time[2] the existence of clusters involving transition metals further to the left in the periodic table has been realized only relatively recently, namely, with Zr_6I_{12}, $(Zr_6Cl_{12})Cl_3$, $Sc(Sc_6Cl_{12})$,[3,4] and $La(La_6I_{12})$.[5] Among these elements those phases involving the dipositive oxidation state of zirconium have been the most studied, and 6–12-type clusters are now known for all three halides. Layered polymorphic forms of the zirconium dihalides are also found, $ZrCl_2$ and evidently $ZrBr_2$ occurring in MoS_2-type structures,[6,7] and ZrI_2 in extensively intergrown monoclinic (α)[8] and orthorhombic (β)[9] structures related to β-$MoTe_2$ and WTe_2, respectively. In the last two compounds the metal atoms are displaced from centers of antiprismatic sites in a CdI_2-like arrangement to form infinite zigzag chains (d(Zr–Zr) = 3.18 Å) between bucked iodine layers. The Zr_6I_{12} cluster polytype described herein is formed at higher temperatures than the other diiodides and is therefore designated γ-ZrI_2. It is the parent structure of the 6–12 clusters, the isostructural Zr_6Cl_{12} and Zr_6Br_{12} having been identified as microcrystalline products by Guinier power diffraction techniques[10] subsequent to preliminary notice[3] of the structure of Zr_6I_{12}.

The reduced zirconium iodides have a particular and continuing importance because of their prime relevance to the stress–corrosion–cracking of zirconium fuel cladding in water-cooled reactors that is evidently caused by fission product iodine.[11] A possible involvement of the abundant fission product cesium has also led to study of reduced phases in the CsI–ZrI_4–Zr system. The relatively oxidized $Cs_3Zr_2I_9$ has been

---

[1] Operated for the U. S. Department of Energy by Iowa State University under Contract No. W-7405-Eng-82. This research was supported by the Office of Basic Energy Sciences, Materials Sciences Division.

[2] Schäfer, H.; von Schnering, H.-G. *Angew. Chem.* **1964**, *76*, 833.

[3] Corbett, J. D.; Daake, R. L.; Poeppelmeier, K. R.; Guthrie, D. H. *J. Am. Chem. Soc.* **1978**, *100*, 652.

[4] Corbett, J. D.; Poeppelmeier, K. R.; Daake, R. L. *Z. Anorg. Allg. Chem.*, in press.

[5] Berroth, K.; Warkentin, E.; Simon, A., unpublished research.

[6] Troyanov, S. I.; Tsirel'nikov, V. I. *Vestn. Mosk. Univ., Ser. 2: Khim.* **1973**, *28*, 67.

[7] Cisar, A.; Corbett, J. D.; Daake, R. L. *Inorg. Chem.* **1979**, *18*, 836.

[8] Guthrie, D. H.; Corbett, J. D. *J. Solid State Chem.* **1981**, *37*, 256.

[9] Corbett, J. D.; Guthrie, D. H. *Inorg. Chem.* **1982**, *21*, 1747.

[10] Imoto, H.; Corbett, J. D.; Cisar, A. *Inorg. Chem.* **1981**, *20*, 145.

[11] Cox, B.; Wood, J. C. "Corrosion Problems in Energy Conversion and Generation"; C. S. Tedmon, Jr., Ed.; Electrochemical Society: New York, 1974; p 275.

0020-1669/82/1321-3290$01.25/0

Table I. Structural Parameters for Zr_6I_{12}[a]

	x	y	z	B_{11}[b]	B_{22}	B_{33}	B_{12}	B_{13}	B_{23}
I1	0.31154 (8)	0.08085 (8)	0.00074 (9)	2.14 (6)	1.83 (6)	1.5 (1)	0.65 (2)	0.23 (2)	0.15 (2)
I2	0.05140 (7)	0.17765 (8)	0.3246 (1)	1.64 (6)	1.96 (6)	1.2 (1)	0.45 (2)	−0.102 (2)	−0.25 (2)
Zr	0.1430 (1)	0.1023 (1)	0.1303 (1)	1.07 (6)	1.01 (6)	0.7 (1)	0.25 (2)	0.02 (2)	0.00 (2)

[a] $R\bar{3}$ ($Z = 3$), $a = 14.502$ (2) Å, $c = 9.996$ (2) Å; $R = 0.109$, $R_w = 0.121$ for 609 reflections, $2\theta \leqslant 49.9°$. The parameters originally published[3] have been converted so as to center the cluster at the origin, consistent with the data for $Zr_6Cl_{12}\cdot K_2ZrCl_6$.[10] (The correct transformation for the y coordinate is $-x - {}^2/_3$.) [b] $T = \exp[-{}^1/_4(B_{11}h^2a^{*2} + B_{22}k^2b^{*2} + B_{33}l^2c^{*2} + 2B_{13}hla^*c^* + 2B_{23}klb^*c^*)]$.

reported already,[12] and we herein describe the synthesis and structure of the cluster $CsZr_6I_{14}$, the structure of which represents a novel interstitial derivative of an arrangement already known for Nb_6Cl_{14}[13] and Ta_6I_{14}.[14]

Experimental Section

Synthetic Studies. Strips of metal rolled from reactor grade crystal bar zirconium, sublimed ZrI_4 prepared from the same stock, and CsI (when appropriate) were used for the syntheses. Preparation and handling of the first two have been described[8] while CsI (Alfa Products) was recrystallized from 0.05 wt % aqueous HI, dried under vacuum at 350 °C, and stored under vacuum. Weighed quantities of the reactants were transferred in the drybox to 9.5 mm o.d. Ta tubing previously closed at one end, the open end was crimped shut, and the container was transferred to a heliarc welder for sealing.

The Zr_6I_{12} phase is generally obtained at higher temperatures than is α,β-ZrI_2 and does not seem to be transported as readily, growing rather as black "gems" either on the metal or in mixture with α,β-ZrI_2 residues. Conditions for the synthesis of $CsZr_6I_{14}$ are similar except that transport occurs. Typical reaction quantities involve 0.4 g of ZrI_4 and 3–8 g of Zr in the form of 5–7 × 0.5 × 0.04 cm strips, plus 0.058 g of CsI (~3:1 mole ratio for ZrI_4:CsI) in the ternary reactions. The use of smaller amounts of metal often results in a metal surface that is blocked from further reaction by a layer of α,β-ZrI_2 or ZrI_2 plus $Cs_3Zr_2I_9$, respectively, for the two compounds investigated. (Blocked systems also exhibit an appreciable pressure of ZrI_3(g), which usually condenses only on the Ta walls when the reaction container is air quenched at the end of a run.) Reaction at temperatures between 820 and 925 °C with or without a temperature gradient for 15–40 days is suitable for both phases. However, Zr_6I_{12} crystals have been recognized as low as 750 °C. The best Zr_6I_{12} gems take the form of well-faceted distorted octahedra with a pair of opposed vertices truncated. These have also been found attached to whiskers of an unknown iodide. The best $CsZr_6I_{14}$ crystals are transported to the 840 °C region and occur as long rectangular prisms which do not fray on cutting (a difference from ZrI_3) and small, black but less reflecting "gem" crystals which have been identified both by Guinier powder data and from tuning single crystals on the diffractometer.

Both phases are visually stable in the air for 1 week or more, and Zr_6I_{12}, to H_2O and aqueous HCl for many minutes.

The oxidized Cs_2ZrI_6 has also been prepared as a reference material by fusion of the appropriate amounts of CsI and ZrI_4. The compound exists as orange-brown, hexagonal-shaped crystals and on the basis of a calculated powder pattern is isostructural with K_2PtCl_6[15] as is Cs_2ZrCl_6.[16] Least-squares refinement of 11 lines measured from a Guinier pattern calibrated with an internal Si standard gave $a = 11.659$ (2) Å.

ESR. Measurements were made at both room and liquid-nitrogen temperature with use of a Bruker ER-220-PSR instrument interfaced to a Nicolet 1170 signal averager.

Data Collection. Crystals of γ-ZrI_2 were mounted in 0.3-mm thin-wall glass capillaries in a glovebox filled with dry nitrogen. A single crystal ~0.25 × 0.35 × 0.45 mm was selected via oscillation photos, and this was indexed by and diffraction data collected on an automated four-circle diffractometer. Hexagonal axes of $a = 14.502$ (2) and $c = 9.996$ (2) Å were obtained from 2θ values for 12 reflections which were tuned on both Friedel-related peaks; very similar values have been obtained from a number of other crystals prepared under a variety of conditions. The extinctions observed indicated rhombohedral centering. Two octants of data (HKL, $H\bar{K}L$, $2\theta \leq 49.9°$) yielded 1119 observed ($I > 3\sigma(I)$) reflections and 609 independent reflections when averaged in Laue symmetry $\bar{3}$.

For $CsZr_6I_{14}$, a crystal ~0.07 × 0.10 × 0.55 mm was similarly handled, and diffraction data were collected for the indicated orthorhombic cell over the octants HKL and $\bar{H}\bar{K}L$ for $2\theta \leq 49.9°$. The C-centered condition was added after 1300 reflections had been checked. Cell parameters of $a = 15.833$ (2) Å, $b = 14.300$ (3) Å, and $c = 12.951$ (2) Å were obtained by refinement of 14 reflections with $28° < 2\theta < 47°$. (For comparison values of 15.822 (2), 14.313 (3), and 12.938 (2) Å were obtained for a different preparation by refinement of 2θ values for 24 lines measured from a Guinier film.) The 2263 observed reflections were reduced and averaged in Laue symmetry *mmm* to 1167 independent data. Additional extinctions indicated space group *Cmca* (No. 64) or *C2cb* (No. 41). A strong statistical test for centricity supported the correctness of the former, as did the structural solution.

Structure Solution. Zr_6I_{12}. Least-squares refinement of positional parameters for two iodine atoms and one zirconium atom in 18-fold general positions that had been deduced by MULTAN[17] yielded $R = 0.22$. At this point a difference map indicated negative peaks at the atom positions. Examination of the data revealed that both low-angle and high-intensity ($F_c > 700$) reflections had F_o values significantly less than F_c, indicating absorption and secondary extinction problems, respectively. Therefore, the raw data were corrected for absorption by TALABS[18] with a crystal shape defined by nine intersecting faces and a value of 178 cm⁻¹ for μ[19] ($0.067 < T < 0.124$). The data were again reduced, averaged, and then refined in EXTLSS,[20] a least-squares program that also allows correction for secondary extinction.

The full-matrix least-squares refinement with isotropic thermal parameters yielded $R = \sum||F_o| - |F_c||/|F_o| = 0.150$. Final least-squares refinement with anisotropic thermal parameters, including reweighting in 10 groups sorted by F_o to allow for a 8.5-fold variation in $\sum w(F_o - F_c)^2$ among these, resulted in converged values of $R = 0.109$, $R_w = [\sum w(|F_o| - |F_c|)^2/\sum w|F_o|^2]^{1/2} = 0.121$. The principal limitation in the residual values appears to be the difficulty in making a precise absorption correction, but the standard deviations are quite respectable.

A final difference map was flat to <0.4% of an atom at the atom positions and at the center of the cluster. Negative regions around iodine atom positions and the center of the cluster integrated to 1–4% of an iodine atom, while the largest positive peaks elsewhere corresponded to ~2% of an iodine atom.

$CsZr_6I_{14}$. Preliminary orientation and diffractometer studies suggested a monoclinic subcell ~4.1 × 4.0 × 12.9 Å and $\beta \approx 120°$, and phasing of the diffraction data with one iodine atom at the origin indicated the presence of approximately close-packed layers of iodine. That this cell represented only the dominant scattering was confirmed by oscillation photographs which revealed additional, weak reflections. Reindexing provided the correct orthorhombic cell on which data were collected. Fourier maps phased with the iodine at the origin enabled the successive location of five more iodine atoms and the zirconium atoms. The initial heavy atom was now surrounded by iodine atoms,

---

(12) Guthrie, D. H.; Meyer, G.; Corbett, J. D. *Inorg. Chem.* **1981**, *20*, 1192.
(13) Simon, A.; von Schnering, H.-G.; Wöhrle, H.; Schäfer, H. *Z. Anorg. Allg. Chem.* **1965**, *339*, 155.
(14) Bauer, D.; von Schnering, H.-G.; Schäfer, H. *J. Less-Common Met.* **1965**, *8*, 388.
(15) Ewing, F. J.; Pauling, L. *Z. Kristallogr., Kristallgeom., Kristallphys., Kristallchem.* **1928**, *68*, 223.
(16) Engel, G. *Z. Kristallogr., Kristallgeom., Kristallphys., Kristallchem.* **1935**, *90*, 341.
(17) Main, P.; Woolfson, M. M.; Germain, F. "MULTAN, a Computer Program for the Automatic Solution of Crystal Structures"; University of York Printing Unit: York, England, 1971.
(18) Scott, J. D., Queens University, Kingston, Ontario, Canada, private communication, 1971.
(19) "International Tables for X-Ray Crystallography", 2nd ed.; Kynoch Press: Birmingham, England, 1962; Vol. III.
(20) Coppens, P.; Hamilton, W. C. *Acta Crystallogr., Sect. A* **1971**, *A26*, 71.

Table II. Structural Parameters for $CsZr_6I_{14}$[a]

	x	y	z	B_{11}	B_{22}	B_{33}	B_{12}	B_{13}	B_{23}
I1	0.12535 (6)	0.08991 (9)	0.25011 (8)	1.34 (6)	1.51 (6)	1.30 (6)	0.10 (3)	−0.41 (3)	−0.27 (3)
I2	0.12574 (6)	0.25726 (7)	0.00643 (8)	1.40 (6)	1.26 (5)	1.38 (5)	0.32 (3)	0.28 (3)	0.17 (3)
I3	0.25	0.3488 (1)	0.25	1.24 (7)	1.54 (7)	1.62 (6)	0.0	−0.40 (4)	0.0
I4	0.0	0.1581 (1)	0.7618 (1)	1.10 (7)	1.69 (7)	1.31 (6)	0.0	0.0	0.39 (4)
I5	0.24730 (8)	0.0	0.0	0.84 (6)	1.92 (7)	1.40 (6)	0.0	0.0	−0.28 (5)
Cs	0.0	0.0	0.0	3.4 (1)	4.9 (2)	3.0 (1)	0.0	0.0	−0.4 (1)
Zr1	0.39420 (9)	0.0643 (1)	0.8922 (1)	0.99 (6)	1.17 (6)	1.05 (6)	−0.08 (4)	−0.09 (4)	0.06 (4)
Zr2	0.0	0.3668 (1)	0.9021 (1)	1.29 (8)	1.29 (8)	1.13 (7)	0.0	0.0	−0.19 (6)

[a] *Cmca*, $a = 15.833$ (2) Å, $b = 14.300$ (3) Å, $c = 12.951$ (2) Å; $R = 0.062$, $R_w = 0.083$ for 1169 reflections, $2\theta \leqslant 49.9°$.

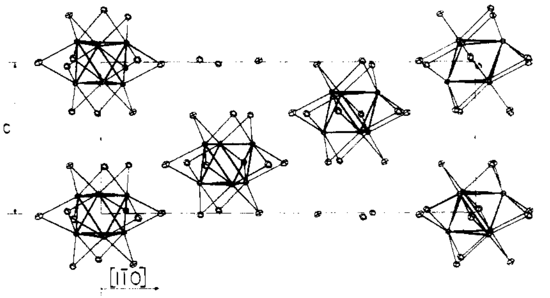

Figure 1. [110] section of the structure of Zr_6I_{12} ($R\bar{3}$). Only the connectivity of the iodine atoms within the metal cluster is shown (50% probability thermal ellipsoids).

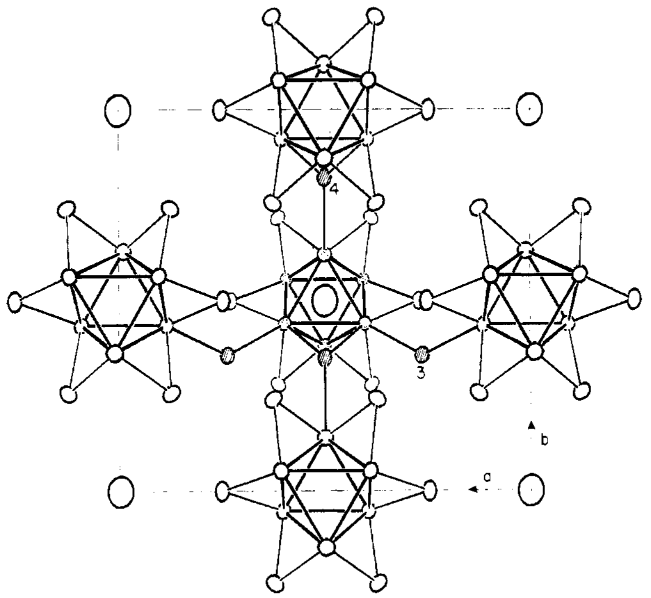

Figure 2. [001] section of the $CsZr_6I_{14}$ structure (*Cmca*) showing cesium (large ellipsoids) and the four clusters centered on the edges of the (001) face. Also included is the metal cluster at the body center of the cell (dotted ellipsoids) and the I3 and I4 atoms (striped), which bridge it to the other clusters. Other iodine atoms that bridge top and bottom faces of metal antiprisms have been omitted for clarity (85% thermal ellipsoids).

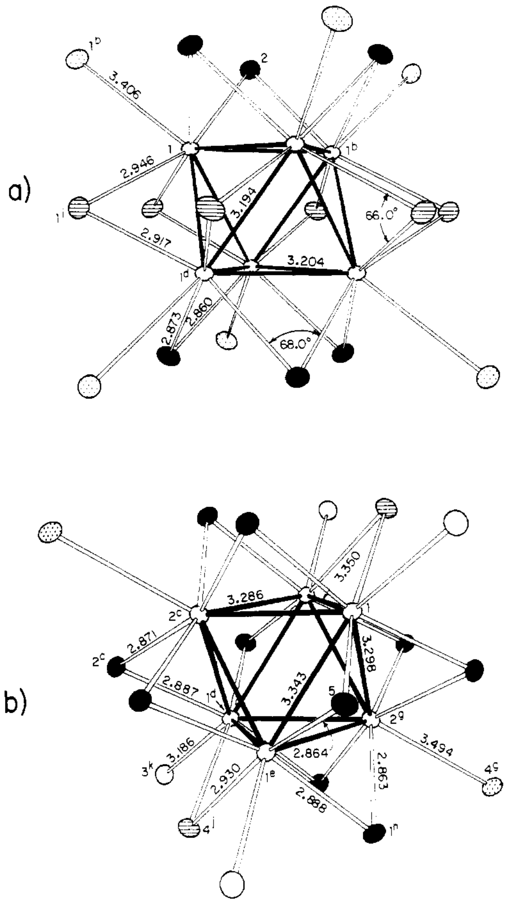

Figure 3. Distances and iodine connectivity in the clusters in (a) Zr_6I_{12} (D_{3d}) and (b) $CsZr_6I_{14}$ (C_{2h}). Solid ellipsoids are I^i, striped are $I^{i\text{-}a}$, dotted are $I^{a\text{-}i}$ from another cluster, and open are $I^{a\text{-}a}$. The atom coding is footnoted in Table III (*c* axes vertical).

and its assignment was changed to that of cesium on the basis of common sense. The data were corrected for absorption by a ϕ-scan method[21] (0–350° in 10° steps, $\mu = 181$ cm^{-1}, $0.62 < T < 0.99$) and were reweighted in fifty groups sorted on F_o. The converged values of R and R_w utilizing anisotropic temperature factors were 0.062 and 0.083, respectively. Integrated intensities for small, positive peaks in the final difference map were judged relative to the corresponding values from the electron density map. The Cs and Zr atom positions in the former as well as nominally empty regions were flat to $Z < \pm 0.5$, while iodine positions showed residuals corresponding to $Z = 2.4$–2.8. A small peak at the center of the cluster in both maps (point symmetry $2/m$) corresponded to $Z = 3$–4. This presumably (but not certainly) arises from errors in the data, as discussed elsewhere.[4]

Results and Discussion

Clusters of Zr_6I_{12} are found in both structures. Final positional and thermal parameters for Zr_6I_{12} and $CsZr_6I_{14}$ are listed in Tables I and II, respectively, while structure factor data are available as supplementary material. Important distances and angles in both structures are given in Table III. Figures 1 and 2 illustrate the cluster packing in the two unit cells while Figure 3 shows the dimensions and iodine connectivity of the clusters in each.

Structure Descriptions. Zr_6I_{12}. The simplest view of the structure of Zr_6I_{12} (γ-ZrI_2) is one of ccp clusters stacked with their $\bar{3}$ axes normal to the layers, as shown in the [110] projection in Figure 1. An alternative close-packed atom description will be considered later. The interconnectivity of these clusters derives from the fact that 12 inner (i) halide atom bridging edges of the metal octahedron leave an appreciable fraction of a hemisphere around each metal atom

---

[21] Karcher, B. A.; Jacobson, R. A., private communication, 1980.

Table III. Important Distances (Å) and Angles (Deg) in Zr_6I_{12} and $CsZr_6I_{14}$[a]

	Zr_6I_{12}		$CsZr_6I_{14}$	
	atoms	dist or angle	atoms	dist or angle
Zr–Zr intralayer	$1\text{–}1^b$	3.204 (2)	$1\text{–}2^c$	3.286 (2)
			$1^d\text{–}1^c$	3.350 (3)
Zr–Zr interlayer	$1\text{–}1^f$	3.194 (1)	$1\text{–}1^e$	3.343 (3)
			$1\text{–}2^g$	3.298 (2)
	$1^b\text{–}1^f$	4.525 (2)	$1\text{–}1^d$	4.733 (3)
			$2^c\text{–}2^g$	4.577 (4)
$Zr\text{–}I^i$	$1^b\text{–}2$	2.860 (2)	1–5	2.864 (2)
	1–2	2.873 (2)	$1^e\text{–}1^h$	2.888 (2)
			$1^d\text{–}2^c$	2.887 (2)
			$2^g\text{–}1^h$	2.863 (2)
			$2^c\text{–}2^c$	2.871 (2)
$Zr\text{–}I^{i\text{-}a}$	$1^d\text{–}1^i$	2.917 (2)	$1^e\text{–}4^j$	2.930 (2)
	$1\text{–}1^i$	2.946 (2)		
$Zr\text{–}I^{a\text{-}i}$	$1\text{–}1^b$	3.406 (2)	$2^g\text{–}4^g$	3.494 (3)
$Zr\text{–}I^a$			$1^d\text{–}3^k$	3.186 (2)
$Zr\text{–}I^i\text{–}Zr$	1–2–1	67.96 (5)	$1^e\text{–}1^h\text{–}2^g$	69.68 (5)
			$1^d\text{–}2^c\text{–}2^c$	69.88 (5)
			$1\text{–}5\text{–}1^e$	71.41 (6)
$Zr\text{–}I^{i\text{-}a}\text{–}Zr$	1–1–1	66.02 (4)	$1^d\text{–}4^j\text{–}1^e$	69.74 (6)
$Zr\text{–}I^a\text{–}Zr'$			$1^d\text{–}3^k\text{–}1'$	134.08 (7)

[a] Superscripts on I refer to bridging functions (i = inner, a = outer) and on atom numbers to symmetry operations given in the following footnotes. [b] $\bar{y}, x-y, z$. [c] $1/2+x, 1/2+y, \bar{z}$. [d] $\bar{x}, \bar{y}, \bar{z}$. [e] $\bar{x}, y, z$. [f] $y, y-x, \bar{z}$. [g] $1/2-x, 1/2+y, z$. [h] $x, 1/2-y, 1/2+3$. [i] $1/3-y, x-y-1/3, z-1/3$. [j] $\bar{x}, 1/2+y, 1/2-z$. [k] $1/2-x, \bar{y}, 1/2+z$.

vacant. Accordingly, the outward-pointing (a (for äusser[2]) or exo) position at each metal in M_6X_{12} (and M_6X_8) clusters is always found to be occupied by another halide. In Zr_6I_{12} this role is filled by iodine atoms in other clusters, such that the six I1 atoms about the waist of each cluster are also more distant to exo positions in other clusters, three above and three below when viewed along [001] (these interactions are not shown in Figure 1). This is completely analogous to the role of the $ZrCl_6^{2-}$ antiprism in bridging to the exo positions of six Zr_6Cl_{12} clusters, three above and three below, in $Zr_6Cl_{12}\cdot M_2ZrCl_6$.[10]

Figure 3a shows the iodine disposition about one Zr_6I_{12} cluster (point symmetry $\bar{3}$ (D_{3d})). The solid I^i atoms are bonded twice to the cluster shown (average d(Zr–I) 2.866 Å) and the six striped $I^{i\text{-}a}$ about the waist, twice to this cluster (d = 2.932 Å) and once to another (d = 3.406 Å), while the dotted atoms $I^{a\text{-}i}$ are the complement of the latter in other clusters. A useful description of the compound taking into account the different iodine atom functionalities is thus $Zr_6I^i{}_6I^{i\text{-}a}{}_{6/2}I^{a\text{-}i}{}_{6/2}$. The cluster is slightly compressed along the $\bar{3}$ azis (Δd(Zr–Zr) = 0.010 Å, 4.5σ), following the higher connectivity of and longer distances to the waist I1 atoms. The Zr–I distances are very comparable to those in $Cs_3Zr_2I_9$, 2.84–2.88 Å, as would be expected since the reduction electrons in such compounds are generally not screening to the nonmetal.[22]

$CsZr_6I_{14}$. This structure is simply described again as approximately ccp Zr_6I_{12} units, now with cesium atoms occupying all octahedral interstices, but the more complex interconnectivity through exo positions that is required by the stoichiometry reduces the symmetry to orthorhombic. Figure 2 shows a (110) section of a portion of the cell contents, namely, the closer Zr_6 units and their waist-bridging iodine atoms, the Cs atoms, and just the bridging connections to the top half of the cluster located below in the body center. A single $Zr_6I_{14}^-$ cluster with all Zr–I interactions is isolated in Figure 3b (point symmetry $2/m$ (C_{2h})). With two more iodine atoms available than before, 10 of 12 edges are now bridged by I^i (solid ellipsoids, 2.878 Å average d(Zr–I)), while I4 is functionally $I^{i\text{-}a}$ (striped, d = 2.930 Å within and 3.494 Å to another cluster) and I3 is two-coordinate $I^{a\text{-}a}$ (open, 3.186 Å). The connectivity description is thus $Cs[Zr_6I^i{}_{10}I^{i\text{-}a}{}_{2/2}I^{a\text{-}i}{}_{2/2}I^{a\text{-}a}{}_{4/2}]$. The weaker bonding of I4 in the exo position of Zr_2 appears to be responsible for a compression of the metal "octahedron" along the Zr2–Zr2 axis, giving eight Zr2–Zr1 distances of 3.292 Å and four Zr1–Zr1 distances around the waist that average 3.347 Å.

There is nothing particularly noteworthy about the nonbonding distances in either structure. Iodine–iodine distances in both give the impression of van der Waals type contacts between neighbors, 3.97–4.08 Å in Zr_6I_{12} and 3.94–4.01 Å in $CsZr_6I_{14}$ save for $I3^{a\text{-}a}$–$I5^i$, 3.89 Å. The iodine polyhedron about cesium consists of a near-square-planar arrangement, two each at 3.824 (2) and 3.916 (2) Å to I4 (above and below) and I5 (in plane), respectively, plus four each to I_1 at 4.01 Å and to I2 at 4.18 Å. The sum of the six-coordinate crystal radii is 3.87 Å.[23]

Except for the cesium atom the structure of $CsZr_6I_{14}$ is the same as that of the binary Nb_6Cl_{14}[13] and Ta_6I_{14},[14] as is seen most easily when the latter representations are converted to the standard setting (*bca*) and the origin shifted by (0, 0, 1/2). The lattice dimensions of Nb_6Cl_{14} are proportioned more nearly as found here, and these two metal octahedra show similar but smaller distortions than in Ta_6I_{14}. The indicated interconnectivity of the clusters in the binary compounds generates holes (obscured in the drawings in the earlier reports) which accommodate the cesium ions in $CsZr_6I_{14}$. Similar derivatives should be possible for these M_6X_{14} phases *provided* the 16-electron clusters can be reduced, a feat that has not been accomplished heretofore in solution let alone in the solid state. The vacancies in Ta_6I_{14} appear relatively large since the Ta–Ta cluster dimensions are 0.4–0.5 Å less and the cell axes differ by only −0.83, +0.14, and −0.45 Å, respectively, relative to those of $CsZr_6I_{14}$ (standard setting). The effect of nonuniform bridging in these differences as a function of cluster and anion is evident.

Metal–Metal Bonding. The average Zr–Zr distances in Zr_6I_{12} and $CsZr_6I_{14}$, 3.20 and 3.31 Å, respectively, are comparable with the 3.205-Å average in the hcp metal, 3.20 Å in $Zr_6Cl_{12}\cdot K_2ZrCl_6$,[10] and 3.21 Å in $Zr_6Cl_{12}Cl_{6/2}$.[4] Although the agreement with the distance in the metal gives a qualitative measure of the bond strength, it is fortuitous since only half the number of electrons are available to bond one-third as many nearest neighbors. A more systematic treatment shows the Pauling bond order per electron pair summed over all Zr–Zr distances in the Zr_6I_{12} cluster is only about 70% of that in the metal.[22] This doubtlessly arises from the hindrance of the metal–metal bonding caused by anion–anion repulsive contacts, also referred to as the matrix effect. The ideal figure for the 6–12 cluster is probably a cube of halide atoms with the metal atoms on or near the faces of the cube. A characteristic of nearly all 6–12 clusters is that the metal positions are significantly inside the halide cube, as can be seen in Figure 3, presumably because repulsions between the nonmetal atoms distort the ideal polyhedron as well as limit the amount of metal–metal bonding. Among the 6–12 halides this effect would be greatest with iodide but the repulsion is at the same time less with the greater zirconium radius, so that the bond orders for Nb_6Cl_{14} and Zr_6I_{12} turn out to be similar. These same nonbonding contacts appear to be the determining factor in the Zr–I^a approach to the clusters (Figure 3).

Twelve and eleven electrons are available for metal–metal binding in Zr_6I_{12} and $CsZr_6I_{14}$, respectively, with the plausible

---

[22] Corbett, J. D. *J. Solid State Chem.* **1981**, *37*, 335.

[23] Shannon, R. D. *Acta Crystallogr., Sect. A* **1976**, *A32*, 751.

assumption that the nonmetal valence band is filled and below that of the Zr_6 group. The 0.1-Å difference in average *d*(Zr–Zr) between these seems rather large for a difference of only $^1/_{12}$ in the number of bonding electrons, although the more unsymmetric bridging in the latter may be important as it probably is with respect to the greater distortion observed for that octahedron. Incidentally, samples of $CsZr_6I_{14}$ prepared in the presence of certain nonmetal impurities have been found to exhibit significantly larger lattice dimensions, as has been observed for $CsNb_6I_{11}H$ relative to $CsNb_6I_{11}$.[24] The structure reported here pertains to a crystal with about the smallest lattice dimensions found. This problem is under further investigation.

A quantitative study of the magnetic susceptibility of these two materials has been prevented by our inability to prepare sufficient amounts of phase-pure samples. Several small samples of each have been studied by ESR spectroscopy at both room and liquid-nitrogen temperatures without the detection of a significant signal. For Zr_6I_{12} the samples amounted to a few milligrams of single crystals. Individual crystals of the cesium salt that came from different preparations were examined under conditions where one spin per cluster would be several orders of magnitude above sensitivity. No explanation for the lack of an observable resonance in the latter is at hand save the usual rationalizations regarding relaxation and broadening. On the other hand a diamagnetic Zr_6I_{12} does seem reasonable, as follows.

The most complete calculations published for M_6X_{12}-type clusters[25] suggest that a strictly octahedral unit with 12 electrons should be paramagnetic, with four electrons in the highest occupied t_{1u} orbital. However, the real cluster exhibits a small trigonal compression, the effect of which would be enhanced by the intercluster bridging role played by the six iodine atoms around the waist. That this is a real distortion is supported by the fact that a significantly greater distortion is seen in $Zr_6Cl_{12}\cdot K_2ZrCl_6$, 3.178 (1) Å between vs. 3.224 (1) Å within the metal triangles perpendicular to the 3-fold axis. In this case the cluster chloride is all Cl^i with $ZrCl_6$ filling the exo positions. Supporting a diamagnetic product are some approximations from extended Hückel calculations on the iodide (ICON8[26] with weighted H_{ij} and valence-state energies estimated by the usual averaging over all terms). No attempt was made to account for the effect of the exo iodine atoms, but protons were positioned 2 Å outside the waist iodine atoms to simulate the effect of their bridging. This gave predominately metal states with occupancies as follows: a_{1g}^2, −8.72; e_u^4, −7.77; a_{2u}^2, −7.52; e_u^4, −7.50; a_{1g}^0, −7.40; e_u^0, −6.14 eV. Other procedures, such as increasing the binding energy of the valence levels of $I^{i\text{-}a}$ by 1–1.5 eV without introduction of H, gave similar energies and a reasonable charge distribution but a smaller gap.

Close-Packed Comparisons. As noted earlier by Imoto[10] these structures as well as some related examples can all be described in a simple and useful way in terms of close-packed layers of nonmetal atoms. This is summarized in Table IV. The structure of γ-ZrI_2 (Zr_6I_{12}) consists of ccp layers of iodine (ABC... or $(c)_3$) with zirconium atoms occupying half the octahedral holes between these in triangular groups of three. These Zr_3 units pair up about a vacant iodine position in the intervening iodine layer to form trigonal-antiprismatic Zr_6 clusters (Figure 1). The displacement of the metal atoms toward one another puckers the iodine layers slightly and leaves one more distant iodine neighbor to each metal, that which has been described as occupying the exo position. The rhombohedral β-Nb_3I_8[27] is a good example of the first stage, the formation of bonded triangular units but with a more extended layering sequence. The previously discovered structure of $Sc(Sc_6Cl_{12})$[3,4] as well as of La_7I_{12}, etc.[5] is generated by the simple addition of scandium (La) atoms to the vacant trigonal-antiprismatic sites in the Zr_6I_{12} structure which lie between the clusters and along their common 3-fold axes. (These centers at 0, 0, $^1/_2$, etc. are marked with a small dot in Figure 1.) There is no evidence for the analogous $Zr_x(Zr_6X_{12})$ phases,[10] the chloride and bromide systems near this stoichiometry instead forming superstructures of layered dihalides.[7]

Table IV. Close-Packed Description of Some 6–12 Cluster Structures

compd	close-packed layer sequence	halide per cluster[e]	additional atoms[f]	substitution[g]
Zr_6X_{12}[a]	*c*	13	none	none
Sc_7Cl_{12}[b]	*c*	13	Sc^{III}	none
Nb_6Cl_{14}, Ta_6I_{14}[c]	*ch*	16	none	vacancy in *c*
$CsZr_6I_{14}$	*ch*	16	none	Cs in *c*
$Zr_6Cl_{12}\cdot K_2ZrCl_6$[d]	*chh*	7	Zr^{IV} between *h*	K in *h*

[a] X = Cl, Br, I; this work and ref 10. [b] References 3 and 4; also ref 5 for La_7I_{12} etc. [c] Nb_6Cl_{14}, ref 13; Ta_6I_{14}, ref 14. [d] Reference 10. [e] Before substitution or removal of halide at the center of the cluster. [f] See text. [g] Other than missing halide at the center of the cluster.

In Nb_6Cl_{14} and Ta_6I_{14} the layering sequence perpendicular to the *c* axis is ABAC... [or $(hc)_2$] and clustering occurs around missing X atoms in, necessarily, the *c* (or A) layers. These *c*[28] layers also exhibit a second halide vacancy, apparently generated by requirements of the halogen bridging. It is this vacant position that is filled by Cs in $CsZr_6I_{14}$. Such a layer composed of waist-bridging atoms I2 and I5, vacancies at the centers of the clusters, and the cesium substituent is the top layer in Figure 2, while portions of the *h* layers make up the top and bottom layers seen in Figure 3b. Occupancy of the cesium sites by halide to form $M_6X_{14}X'$ instead would seem unreasonable since halide evidently always occurs either coordinated to edges or faces of the metal octahedra or bridging between exo positions rather than "free" with only halide neighbors. (The resulting M_6X_{15} has a more plausible structure, $M_6X^i_{12}X^a_{6/2}$.[29]) Finally, $K_2ZrCl_6\cdot Zr_6Cl_{12}$ behaves analogously with respect to cluster formation, showing potassium substitution in two-thirds of the chlorine layers together with octahedral zirconium(IV) therebetween, the entire assembly generating a more extended layering sequence.

Although binary, halogen-bridged clusters containing octahedra of metals from transition groups 5 and 6 with 14–24 binding electrons have been known for many years, examples from earlier groups have appeared only recently, namely, the 9-electron Zr_6Cl_{15}, Sc_7Cl_{12}, and La_7I_{12} and the 12-electron example described here plus Zr_6Cl_{12} and Zr_6Br_{12}. The late arrival of these electron-poor examples can be partly attributed to the fact that suitable reaction containers have only recently been available, but kinetic limitations for their formation also appear relatively significant. On the other hand, thermodynamic stability does not appear to be a particular problem if the decomposition reaction is limited to disproportionation rather than reduction of some solvent. Attainment of all of the particularly stable electronic arrangements in simple binary systems does not seem highly probable, particularly in view

---

(24) Imoto, H.; Corbett, J. D. *Inorg. Chem.* **1980**, *19*, 1241.

(25) Robbins, D. J.; Thomson, A. L. *J. Chem. Soc., Dalton Trans.* **1972**, 2350.

(26) Summerville, R. H.; Hoffmann, R. *J. Am. Chem. Soc.* **1976**, *98*, 7240 and references therein.

(27) Simon, A.; von Schnering, H.-G. *J. Less-Common Met.* **1966**, *11*, 31.

(28) Misprinted C in ref 10, page 150.

(29) Bauer, D.; von Schnering, H.-G. *Z. Anorg. Allg. Chem.* **1968**, *361*, 259.

of the rather specific requirements for halide binding both within and between the clusters. For this reason ternary systems have also been under investigation, leading to the discovery of $CsNb_6I_{11}$,[24] the present $CsZr_6I_{14}$ as sort of an intercalate of a known structure type, and, recently, the analogous $NaNb_6Cl_{15}$ with the Nb_6Cl_{15} structure and a new structure type for $CsNb_6Cl_{15}$.[30] Obviously the use of a higher-valent second metal, especially with the electron-poorer clusters, seems attractive, for example, with MZr_6I_{14}, where M = Ba would give a cluster isoelectronic with Zr_6I_{12}. Doubtlessly, less obvious derivatives will be found as well.

Acknowledgment. The authors are indebted to R. A. Jacobson for continued crystallographic advice, to R. G. Barnes and D. T. Torgeson for assistance in ESR measurements, and to D. M. P. Mingos and P. Minshall for assistance in the computation, time for which was provided by the Inorganic Chemistry Laboratory, Oxford University.

Registry No. Zr_6I_{12}, 66908-75-6; $CsZr_6I_{14}$, 82456-16-4; ZrI_4, 13986-26-0; Zr, 7440-67-7; CsI, 7789-17-5.

Supplementary Material Available: A listing of structure factor amplitudes for Zr_6I_{12} and $CsZr_6I_{14}$ (6 pages). Ordering information is given on any current masthead page.

---

[30] Imoto, H.; Simon, A., private communication, 1981.

Contribution from the Department of Chemistry and Materials Research Laboratory, University of Illinois, Urbana, Illinois 61801, and the Department of Chemistry, State University of New York at Buffalo, Buffalo, New York 14214

Vibrational Study and Crystal Structure of (μ-Hydrido)(μ-formato)decacarbonyltriosmium, $(\mu\text{-H})(\mu\text{-O}_2\text{CH})\text{Os}_3(\text{CO})_{10}$[1]

JOHN R. SHAPLEY,*[2] GEORGE M. ST. GEORGE,[2] MELVYN ROWEN CHURCHILL,*[3] and FREDERICK J. HOLLANDER[3]

Received December 16, 1981

The formate compounds $(\mu\text{-H})(\mu\text{-O}_2{}^{12}\text{CH})\text{Os}_3(\text{CO})_{10}$, $(\mu\text{-H})(\mu\text{-O}_2\text{CD})\text{Os}_3(\text{CO})_{10}$, and $(\mu\text{-H})(\mu\text{-O}_2{}^{13}\text{CH})\text{Os}_3(\text{CO})_{10}$ have been prepared from the reactions of $\text{Os}_3(\text{CO})_{10}(\text{C}_8\text{H}_{14})_2$ with the acids $\text{H}^{12}\text{CO}_2\text{H}$, DCO_2H, and $\text{H}^{13}\text{CO}_2\text{H}$, respectively. Infrared data on the formate ligand vibrational modes in these compounds were collected and assigned. The assignments were supported by an approximate normal-coordinate analysis of the vibrationally isolated formate group. The carbon–hydrogen stretching frequency is unusually high for a formate complex, which is interpreted to indicate considerable charge transfer to the $\text{Os}_3(\text{CO})_{10}$ unit. Comparison of the formate frequencies found for the molecular complexes $(\mu\text{-H})(\mu\text{-O}_2\text{CH})\text{Os}_3(\text{CO})_{10}$ and $(\mu\text{-H})(\mu\text{-O}_2\text{CD})\text{Os}_3(\text{CO})_{10}$ with those observed for chemisorbed HCO_2– and DCO_2– on Ag(110) by Sexton and Madix shows good overall correspondence. The complex $(\mu\text{-H})(\mu\text{-O}_2\text{CH})\text{Os}_3(\text{CO})_{10}$ crystallizes in the triclinic space group $P\bar{1}$ with a = 7.9683 (15) Å, b = 15.316 (2) Å, c = 15.744 (2) Å, α = 65.834 (11)°, β = 80.100 (13)°, γ = 88.184 (14)°, V = 1725.4 (5) Å^3, and Z = 4 (i.e., *two* molecules per asymmetric unit). Diffraction data (Mo Kα, 2θ = 445°) were collected with a Syntex $P2_1$ automated four-circle diffractometer, and the structure was solved by conventional methods. All nonhydrogen atoms were located, and final discrepancy indices were R_F = 4.75% and R_{wF} = 3.25% for the 4538 unique reflections. Each independent molecule in the unit cell contains a triangular triosmium core in which one osmium atom (Os(3)) is linked to four terminal carbonyl ligands; the other two osmium atoms (Os(1) and Os(2)) are each linked to three terminal carbonyl ligands, are bridged diaxially by a formate moiety, and are bridged diequatorially by a hydride ligand (which was *not* located directly but which had an apparent position). Each molecule possesses approximate C_s symmetry. The Os_3 plane makes an obtuse angle (average 98.6°) with the O(1)–Os(1)–Os(2)–O(2) "coordination plane"; the formate ligand (defined by O(1)–C(1)–O(2)) bends outward by a further small amount (average 5.3°). The bridged osmium–osmium distances (average Os(1)–Os(2) 2.908 Å) are 0.033 Å larger than the nonbridged intermetallic distances (average 2.875 Å).

Introduction

The metal-catalyzed decomposition of formic acid has been studied extensively, and chemisorbed formate is implicated as an intermediate.[4] Infrared spectroscopy, either in the transmission mode for supported metals[5] or in the reflectance mode for metal films,[6] has been used to observe surface formate species. Recently, however, electron energy loss spectroscopy has been applied to the study of formate species formed on Cu(100)[7] and Ag(110)[8] crystal surface planes. Comparison of vibrational data represents one of the few means of examining a particular moiety both as a chemisorbate on a metal surface and as a ligand in a structurally well-characterized molecular metal complex.[9] Since the title compound[10] contains only carbonyl ligands in addition to the elements of formic acid, it appeared to be an especially suitable model compound. We have prepared isotopically labeled versions of the compound and have obtained and analyzed infrared data on the formate ligand in order to allow a comparison with vibrational data on surface formate species.

From a purely structural point of view, we have examined a number of $(\mu\text{-H})(\mu\text{-L})\text{O}_3(\text{CO})_{10}$ compounds of type I, in which the bridging hydride ligand and the ligand L occupy sites intermediate between axial and equatorial. These include $(\mu\text{-H})_2\text{Os}_3(\text{CO})_{10}$,[11] $(\mu\text{-H})(\mu\text{-CHCH}_2\text{PMe}_2\text{Ph})\text{Os}_3(\text{CO})_{10}$,[15]

---

[1] This paper is considered to be part 23 in the series "Structural Studies on Polynuclear Osmium Carbonyl Hydrides". For previous parts see: (a) Part 20: Churchill, M. R.; Bueno, C.; Kennedy, S.; Bricker, J. C.; Plotkin, J. S.; Shore, S. G. *Inorg. Chem.* **1982**, *21*, 627. (b) Part 21: Shapley, J. R.; Samkoff, D. E.; Bueno, C.; Churchill, M. R. *Ibid.* **1982**, *21*, 634. (c) Part 22: Churchill, M. R.; Bueno, C.; Hsu, W. L.; Plotkin, J. S.; Shore, S. G. *Ibid.* **1982**, *21*, 1958.

[2] University of Illinois.

[3] State University of New York at Buffalo.

[4] For a recent review see: Madix, R. J. *Adv. Catal.* **1980**, *29*, 1.

[5] Little, L. H. "Infrared Spectra of Adsorbed Species"; Academic Press: New York, 1966.

[6] Ito, M.; Suetaka, W. *J. Catal.* **1978**, *54*, 13 and references therein.

[7] Sexton, B. A. *Surf. Sci.* **1979**, *88*, 319.

[8] Sexton, B. A.; Madix, R. J. *Surf. Sci.* **1981**, *105*, 177.

[9] For a recent review, see: Muetterties, E. L.; Rhodin, T. N.; Band, E.; Brucker, C. F.; Pretzer, W. R. *Chem. Rev.* **1979**, *79*, 91.

[10] Bryan, E. G.; Johnson, B. F. G.; Lewis, J. *J. Chem. Soc., Dalton Trans.* **1977**, 1328.

[11] Part 5: Churchill, M. R.; Hollander, F. J.; Hutchinson, J. P. *Inorg. Chem.* **1977**, *16*, 2697. See also ref 12–14.

0020-1669/82/1321-3295$01.25/0